

Synthesis, Spectroscopy, Bonding and Structure in Phosphido Bridged Bimetallics Derived from Bent Metallocenes of Molybdenum and Tungsten and from Group 6 Metal Carbonyls

Christophe Barré, Patrick Boudot, Marek M. Kubicki,* and Claude Moïse

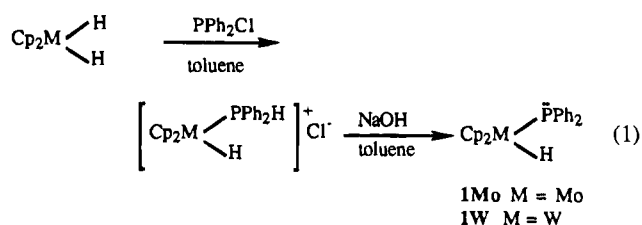
Laboratoire de Synthèse et d'Electrosynthèse Organométalliques (URA CNRS 1685), Faculté des Sciences, Université de Bourgogne, 6 Bd Gabriel, 21000 Dijon, France

Received January 21, 1994[®]

Terminal phosphido complexes $Cp_2M(H)PPh_2$ (**1**, $M = Mo, W$) react with group 6 metal carbonyls $M'(CO)_5$ (THF) ($M' = Cr, Mo, W$) leading to the monophosphido-bridged compounds $Cp_2M(H)(\mu-PPh_2)M'(CO)_5$ (**2**) and $Cp_2M(\mu-PPh_2, H)M'(CO)_4$ (**3**) in high yields. Complexes **3** are also easily obtained in reactions of **1** with $M'(CO)_4L_2$ ($L_2 = nbd$ or pip_2). New complexes **2** and **3** were studied by IR, 1H and ^{31}P NMR spectroscopies, and EHMO calculations were performed on their models, as well as on that of metallophosphines **1**. A very good agreement of results obtained by different methods is observed, in particular in that which concerns the fluctuation of electron density between different molecular fragments. These results show that $M'(CO)_4$ fragments in complexes **3** are able to accept more electron density than the $M'(CO)_5$ units in complexes **2**. The W–W distance of 3.271(1) Å found by X-ray analysis of $Cp_2W(\mu-PPh_2, H)W(CO)_4$ is considered as indicative of a metal ($18e^-$)–metal ($18e^-$) interaction. The electronic nature of the “transition metal gauche effect” is discussed on the basis of EHMO calculations.

The chemistry of transition-metal complexes with diorganophosphido ligands has attracted much attention due to the ease with which steric and electronic factors can be tuned. It has been shown that pyramidal terminal phosphido complexes (metallophosphines) easily form binuclear compounds, and an extensive literature covers this topic.^{1–4} It has also been suggested that these complexes may exhibit an exceptional nucleophilicity⁵ which was attributed by Gladysz to the existence of the “gauche effect”⁶ in transition metal chemistry. We expected an efficient operation of this “gauche effect” in the chiral niobio-phosphine $Cp_2Nb(CO)P^iPrPh$ ⁷ and suggested its potential validity in other metallophosphines derived from bent metallocenes (metal d^2). Recently, Darensbourg and co-workers studied the aspects of conformational preferences of ligands in bent metallocene–thiolate complexes of Ti⁸ and Nb,⁹ and extended Huckel calculations were carried out by Calhorda, Dias et al. for similar purposes.¹⁰ We have already reported on the easy synthesis of molybdenum and tungsten terminal metallo-

phosphido complexes $Cp_2M(H)PPh_2$ **1**^{11,12} from Cp_2MH_2 and PPh_2Cl (eq 1).



There are three potential sites of reactivity in complexes **1**: the hydride ligand, the phosphorus lone pair, and the lone pair of the metal (M^{IV} , d^2). Thus it may be expected that these complexes can exhibit a rich chemistry and give various phosphido- and/or hydrido-bridged polynuclear structures. In particular, the singly bridged μ -phosphido binuclear complexes without a metal–metal bond and without other bridges should be easily formed. A very limited number of isolated and characterized complexes of this type has been reported. These include a diethylphosphido-bridged Hf/Fe¹³ complex, the diphenylphosphido-bridged bimetallics of Ru/Pt,¹⁴ Mo/Mo, W/W,¹⁵ W/Re,^{16,17} Fe/W/M' ($M' = Cr, Mo, W$),¹⁸ and Nb, Ta/M' ($M' = Cr, Mo, W$),¹⁹ as well as the PX_2 ($X = F, Cl$) bridged Cr/Cr, Cr/W, and W/W systems.²⁰

The first X-ray structure determination of singly bridged μ -phosphido compound derived from a bent metallocene,

[®] Abstract published in *Advance ACS Abstracts*, November 15, 1994.

- (1) *Phosphorus-31 NMR Spectroscopy in Stereochemical Analysis*; Verkade, J. G., Quin, L. D., Eds.; Methods in Stereochemical Analysis 8; VCH Publishers Inc.: Deerfield Beach, FL, 1987: (a) Carty, A. J.; MacLaughlin, S. A.; Nucciarone, D. Chapter 16. (b) Chesnut, D. B. Chapter 5. (c) Verkade, J. G.; Mosbo, J. A. Chapter 13.
- (2) Stephan, D. W. *Coord. Chem. Rev.*, **1989**, *95*, 41.
- (3) Baker, R. T.; Fultz, W. C.; Marder, T. B.; Williams, I. D. *Organometallics* **1990**, *9*, 2357.
- (4) Casey, C. P.; Bullock, R. M. *Organometallics* **1984**, *3*, 1102.
- (5) Buhro, W. E.; Zwick, B. D.; Georgiou, S.; Hutchinson, J. P.; Gladysz, J. H. *J. Am. Chem. Soc.* **1988**, *110*, 2427 and references therein.
- (6) Jolly, W. L. *Acc. Chem. Res.* **1983**, *16*, 310.
- (7) Bonnet, G.; Kubicki, M. M.; Moïse, C.; Lazzaroni, R.; Salvadori, P.; Vitulli, G. *Organometallics* **1992**, *11*, 964.
- (8) Darensbourg, M. Y.; Pala, M.; Houliston, S. A.; Kidwell, K. P.; Spencer, D.; Chojnacki, S. S.; Reibenspies, J. H. *Inorg. Chem.* **1992**, *31*, 1487.
- (9) Darensbourg, M. Y.; Bischoff, C. J.; Pala, M.; Houliston, S. A.; Reibenspies, J. H. *J. Am. Chem. Soc.* **1990**, *112*, 6905.
- (10) Calhorda, M. J.; De C. T. Carrondo, M. A. A. F.; Dias, A. R.; Frazao, C. F.; Hursthouse, M. B.; Martinho Simoes, J. A.; Teixeira, C. *Inorg. Chem.* **1988**, *27*, 2513.
- (11) Kubicki, M. M.; Kergoat, R.; Cariou, M.; Guerschais, J. E.; L'Haridon, P. *J. Organomet. Chem.* **1987**, *322*, 357.

- (12) Barré, C.; Kubicki, M. M.; Moïse, C. *Inorg. Chem.* **1990**, *29*, 5244.
- (13) Baker, R. T.; Tulip, T. H.; Wreford, S. S. *Inorg. Chem.* **1985**, *24*, 1379.
- (14) Powell, J.; Fuchs, E.; Gregg, M. R.; Phillips, J.; Stainer, M. V. R. *Organometallics* **1990**, *9*, 387.
- (15) Shyu, S.-G.; Calligaris, M.; Nardin, G.; Wojcicki, A. *J. Am. Chem. Soc.* **1987**, *109*, 3617.
- (16) Mercer, W. C.; Whittle, R. R.; Burkhart, E. W.; Geoffroy, G. L. *Organometallics* **1985**, *4*, 68.
- (17) Mercer, W. C.; Geoffroy, G. L.; Rheingold, A. L. *Organometallics* **1985**, *4*, 1418.
- (18) (a) Shyu, S.-G.; Lin, P.-J.; Wen, Y.-S. *J. Organomet. Chem.* **1993**, *443*, 115. (b) Shyu, S.-G.; Hsu, J.-Y.; Wen, Y.-S. *J. Organomet. Chem.* **1993**, *453*, 97. (c) Shyu, S.-G.; Hsu, J.-Y.; Lin P.-J.; Wu W.-J.; Peng S.-M.; Lee G.-H.; Wen, Y.-S. *Organometallics* **1994**, *13*, 1699.

Table 1. Crystallographic Data for $\text{Cp}_2\text{W}(\mu\text{-PPh}_2\text{H})\text{W}(\text{CO})_4$

formula: $\text{C}_{26}\text{H}_{21}\text{O}_4\text{PW}_2$	fw = 796.13
$a = 15.724(7)$ Å	space group: $P2_1/n$ (No. 14)
$b = 13.849(2)$ Å	$d_{\text{calc}} = 2.247$ g cm $^{-3}$
$c = 11.521(2)$ Å	$\lambda = 0.71073$ Å
$\beta = 110.30(2)^\circ$	$\mu(\text{Mo K}\alpha) = 100.8$ cm $^{-1}$
$V = 2353.2$ Å 3	$R(F) = 0.036^a$
$Z = 4$	$R_w(F) = 0.047^b$
$T = 20$ °C	GOF = 3.870

$^a R(F) = \sum ||F_o| - |F_c|| / \sum |F_o|$. $^b R_w(F) = \{\sum w(|F_o| - |F_c|)^2 / \sum w|F_o|^2\}^{1/2}$ where $w = [\sigma^2(F_o)]^{-1}$ and $\sigma(F_o) = [\sigma^2(F_o^2) + (0.07F_o^2)^2]^{1/2}$.

$\text{Cp}_2\text{Mo}(\text{H})(\mu\text{-PPh}_2)\text{Mn}(\text{CO})_2\text{Cp}$, showed the largest M–P–M angle observed to date (124.5°)¹² confirming the exceptional fluxionality of the PR_2 bridge suggested by Carty.²¹

In this paper we describe the results obtained in the reactions of complexes **1** with group 6 metal carbonyls. An approach to the nature of the “transition metal gauche effect” and its chemical consequences, as well as the electronic behavior of different fragments in mono- and dinuclear complexes, will be also discussed on the basis of EHMO calculations.

Experimental Section

All reactions were carried out under an argon atmosphere by using standard Schlenk techniques. Solvents were distilled under argon from sodium and benzophenone immediately before use. Column chromatography was supported with silica gel (70–230 mesh, THF). Elemental (C, H) analyses were performed by “Service Central d’Analyse du CNRS” (Vernaison) and are given in the supplementary material.

IR spectra were recorded in THF solutions on a Perkin–Elmer 589B spectrophotometer and ^1H and ^{31}P NMR spectra on JEOL FX100 and Bruker WM 400 spectrometers; chemical shifts are given relative to TMS and H_3PO_4 .

$\text{Cp}_2\text{M}(\text{H})(\text{PPh}_2)$ ($\text{Cp} = \text{C}_5\text{H}_5$; $\text{M} = \text{Mo}$, **1Mo**, $\text{M} = \text{W}$, **1W**),¹² $\text{M}'(\text{CO})_4^-$ (nbd),²² and $\text{M}'(\text{CO})_4(\text{pip})_2$ ²³ were prepared according to the procedures described in literature. $\text{Cr}(\text{CO})_5\text{THF}$ was prepared by the method indicated in literature.²⁴ First 0.43 g (1.95 mmol) of $\text{Cr}(\text{CO})_6$ was dissolved in 100 mL of THF. This colorless solution was irradiated with a UV lamp, HANAU TQ 150. The reaction was monitored by IR in the carbonyl stretching region. The bands of $\text{Cr}(\text{CO})_5\text{THF}$ are 2073 (w), 1937 (vs), and 1895 (m, s) cm^{-1} and that of $\text{Cr}(\text{CO})_6$ is at wavenumber 1980 (vs) cm^{-1} . The irradiation was stopped when the intensity of $\text{Cr}(\text{CO})_6$ band was equal to or lower than the medium–strong 1895 cm^{-1} band of $\text{Cr}(\text{CO})_5\text{THF}$. The necessary time of irradiation was about 2.5 h. The estimated yield of $\text{Cr}(\text{CO})_5\text{THF}$ was 80% (1.56 mmol). However, the real yield may be lower, because the estimation of the ratios of products from IR is less accurate than for example from ^1H NMR data. Thus, an excess of resulting yellow solution of $\text{Cr}(\text{CO})_5\text{THF}$ was used in further reactions with metallophosphines **1**. Two new and well separated bands (2016 (w) and 1835 (m) cm^{-1}) appear upon prolonged irradiation. These bands are assigned to $\text{Cr}(\text{CO})_4(\text{THF})_2$. Thus, any solution exhibiting a detectable amount of $\text{Cr}(\text{CO})_4(\text{THF})_2$ was thrown back. The THF solutions of $\text{Mo}(\text{CO})_5\text{THF}$ (yellow-green) and of $\text{W}(\text{CO})_5\text{THF}$ (yellow) were prepared in similar manner, but the needed times of irradiation were about 5 and 1.5 h, respectively.

Synthesis. Reactions of 1(Mo,W) with Metal Carbonyls. In a typical operation, a 30% excess of $\text{Cr}(\text{CO})_5(\text{THF})$ in THF was added at room temperature to a THF solution of 0.5 g (1.2 mmol) of **1Mo** in 30 mL of THF, and the mixture was stirred for 1 h. During this time the solution turned from yellow to deep orange. The solvent was removed under vacuum, and the resulting solid was washed with pentane, extracted with toluene, and chromatographed. The **2MoCr** complex was obtained in ca. 35% yield (based on **1Mo**) from the first orange band eluted with toluene, and the **3MoCr** complex was

Table 2. Positional Parameters and Their Estimated Standard Deviations for $(\text{Cp})_2\text{W}(\mu\text{-PPh}_2\text{H})\text{W}(\text{CO})_4^a$

atom	x	y	z	B (Å 2)
W1	0.18848(4)	0.22395(4)	0.50438(5)	2.31(1)
W2	0.31347(4)	0.03043(5)	0.59321(5)	2.31(1)
P	0.2203(2)	0.0837(3)	0.3835(3)	2.07(7)
O1	0.4044(9)	0.021(1)	0.878(1)	4.9(3)
O2	0.4047(8)	−0.1642(9)	0.561(1)	5.3(3)
O3	0.4999(8)	0.134(1)	0.623(1)	6.0(4)
O4	0.1582(8)	−0.105(1)	0.612(1)	6.2(4)
C1	0.370(1)	0.026(1)	0.772(1)	4.0(3)
C2	0.370(1)	−0.089(1)	0.569(2)	3.4(4)
C3	0.428(1)	0.099(1)	0.603(2)	4.2(4)
C4	0.215(1)	−0.052(1)	0.606(1)	4.0(4)
C11	0.059(1)	0.285(1)	0.517(2)	5.4(4)
C12	0.105(1)	0.249(1)	0.631(2)	4.4(4)
C13	0.501(1)	0.148(1)	0.614(1)	4.2(4)
C14	0.069(1)	0.123(1)	0.493(2)	4.2(4)
C15	0.034(1)	0.212(2)	0.423(2)	4.9(5)
C16	0.319(1)	0.313(1)	0.572(2)	4.9(5)
C17	0.309(1)	0.282(1)	0.457(2)	3.8(4)
C18	0.230(1)	0.324(1)	0.379(2)	3.7(4)
C19	0.193(1)	0.382(1)	0.443(2)	5.2(5)
C20	0.254(1)	0.374(1)	0.575(2)	5.1(5)
C21	0.1201(9)	0.013(1)	0.286(1)	2.3(3)
C22	0.126(1)	−0.090(1)	0.297(1)	3.1(3)
C23	0.056(1)	−0.143(1)	0.224(2)	3.4(4)
C24	−0.017(1)	−0.104(1)	0.140(2)	3.5(4)
C25	−0.023(1)	−0.004(1)	0.126(2)	4.5(4)
C26	0.049(1)	0.052(1)	0.202(2)	3.4(4)
C27	0.2710(9)	0.110(1)	0.265(1)	2.9(3)
C28	0.3605(9)	0.079(1)	0.288(1)	3.0(3)
C29	0.399(1)	0.098(1)	0.193(1)	3.6(3)
C30	0.352(1)	0.143(1)	0.088(1)	3.3(3)
C31	0.265(1)	0.178(1)	0.069(1)	3.3(4)
C32	0.223(1)	0.162(1)	0.153(1)	3.7(4)
CP1	0.0744	0.2034	0.5356	
CP2	0.2610	0.3350	0.4852	

^a CP1 and CP2 are the gravity centers of C11–C15 and C16–C20 rings, respectively. *B* values for anisotropically refined atoms are given in the form of the isotropic equivalent displacement parameter defined as: $(4/3)[a^2B(1,1) + b^2B(2,2) + c^2B(3,3) + ab(\cos \gamma)B(1,2) + ac(\cos \beta)B(1,3) + bc(\cos \alpha)B(2,3)]$.

recovered (ca. 35% yield) from the second deep orange band eluted with THF. The similar protocol applied to $\text{M}'(\text{CO})_5(\text{THF})$ ($\text{M}' = \text{Mo}, \text{W}$) gave **2MoM'** in ca. 45% and **3MoM'** in ca. 15% yields.

Refluxing of **1Mo** with $\text{Cr}(\text{CO})_5(\text{THF})$ in THF for 2 h led after washing of the crude product with pentane to a pure **3MoCr** in 95% yield (based on **1Mo**). Irradiation (UV lamp HANAU TQ 150) of the mixture of **1Mo** with $\text{M}'(\text{CO})_5(\text{THF})$ ($\text{M}' = \text{Mo}, \text{W}$) gives after workup (chromatography) the complexes **3Mo(Mo,W)** in ca. 70% yield and only the traces of **2Mo(Mo,W)** are recovered. Analogous reactions of **1(Mo,W)** with $\text{M}'(\text{CO})_4(\text{nbd})$ or $\text{M}'(\text{CO})_4(\text{pip})_2$ in THF led directly to the complexes **3(Mo,W)M'** isolated in similar yields.

X-Ray Structure Determination. Crystals of $\text{Cp}_2\text{W}(\mu\text{-PPh}_2\text{H})\text{W}(\text{CO})_4$ (**3WW**) suitable for X-ray analysis were grown from acetone. A deep orange irregularly shaped crystal (approximate dimensions 0.15 × 0.1 × 0.1 mm) was mounted on an Enraf–Nonius CAD4 diffractometer. The pertinent crystallographic data are summarized in Table 1. The unit cell was determined and refined from 25 randomly selected reflections obtained by use of the CAD4 automatic routines. Intensities were corrected for Lorentz and polarization effects and an empirical absorption correction (ψ scan) was made. All calculations were carried out by use of the Enraf–Nonius SDP package with neutral-atom scattering factors. The structure was solved and refined by conventional three-dimensional Patterson, difference Fourier and full-matrix least squares methods. All nonhydrogen atoms were refined with anisotropic thermal parameters. The positions of hydrogen atoms (except those of the bridging hydride) were calculated by the HYDRO program of SDP. These atoms were ridden on the carbon atoms bearing them and included in the final calculations with B_{iso} fixed at the values equal to 1.3 B_{eq} for the corresponding carbon atoms. The coordinates of nonhydrogen atoms are given in Table 2.

(19) Bonnet, G.; Lavastre, O.; Leblanc, J.-C.; Moïse, C. *New J. Chem.* **1988**, 12, 551.

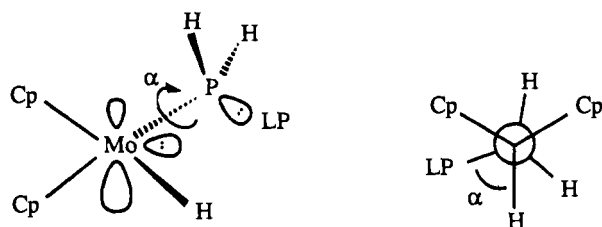
(20) Malish, W.; Panster, P. *Angew. Chem., Int. Ed. Engl.* **1977**, 16, 408.

(21) Carty, A. J. *Adv. Chem. Ser.* **1982**, 196, 163.

(22) Bennett, M. A.; Pratt, L.; Wilkinson, G. J. *Chem. Soc. A* **1961**, 2037.

(23) Darensbourg, D. J.; Kump, R. L. *Inorg. Chem.* **1978**, 17, 2680.

Scheme 1

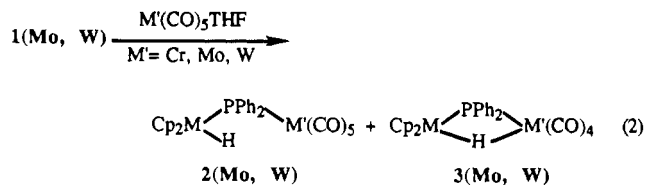


EHMO Calculations. Extended Hückel molecular orbital calculations²⁵ were carried out on the model complexes with $M = M' = \text{Mo}$ and with PH_2 bridge instead that of PPh_2 . The FORTICON8^{25d} program was used for the study of "gauche effect" in $(\text{C}_5\text{H}_5)_2\text{Mo}(\text{H})(\text{PH}_2)$ with following metric parameters: CP (gravity center of C_5 ring)– $\text{Mo} = 2.0 \text{ \AA}$, $\text{Mo–P} = 2.6 \text{ \AA}$, $\text{Mo–H} = 1.7 \text{ \AA}$, $\text{P–H} = 1.4 \text{ \AA}$, $\text{CP–Mo–CP} = 142^\circ$, $\text{P–Mo–H} = 82^\circ$, $\text{Mo–P–H} = 108^\circ$, and $\text{H–P–H} = 102^\circ$. Weighted H_{ij} formula were applied with charge iteration conducted for all atoms according to $H_{ij} = H_{ij}^0 + (\text{sense}) \times (\text{charge})$.²⁶ The dihedral angle $\alpha(\text{H–Mo–P/Mo–P–LP})$ ($\text{LP} = \text{phosphorus lone pair}$) (Scheme 1) was allowed to rotate from 0° to 180° , spanning all possible conformations and relative orientations of both lone pairs. Three molecular orbitals with a total participation of the phosphorus 3s and 3p atomic orbitals higher than 75% and with a contributions of the atoms bound to phosphorus (Mo and H) lower than 15% were considered as representing the phosphorus LP and were used for estimation of the energy of this lone pair and of its s/p character.²⁷ The interactions between the Cp_2Mo and $(\text{PH}_2)(\text{H})\text{Mo}(\text{CO})_n$ ($n = 4, 5$) fragments, as well as between the $\text{Cp}_2\text{Mo}(\text{H})(\text{PH}_2)$ and $M'(\text{CO})_n$ ($n = 4, 5$) ones have been considered for estimation of electronic charges retained on different fragments of the molecules **1**, **2** and **3**. These calculations have been performed with the EH program contained in CACAO package.²⁸ The geometry corresponding to a stable conformation of metallophosphine ($\alpha = 70^\circ$, "gauche effect") was adopted for a model of **1**, that of **2** was extrapolated from the structure of $\text{Cp}_2\text{Mo}(\text{H})(\mu\text{-PPh}_2)\text{Mn}(\text{CO})_2\text{Cp}^{12}$ (hereafter abbreviated to as **2MoMn**) and the parameters found in the structure of **3WW** reported here were used for a model of **3**.

Results

Chemistry. The terminal phosphido complexes **1**(Mo, W) react instantaneously at room temperature with group 6 metal ($M' = \text{Cr}, \text{Mo}, \text{W}$) carbonyls previously irradiated in THF solutions. These reactions lead to the mixtures of monobridged and dibridged μ -phosphido complexes **2** and **3** (eq 2).

The mixtures of **2**(Mo, W) M' and **3**(Mo, W) M' ($M' = \text{Cr}, \text{Mo}, \text{W}$) are easily separated by chromatography. The complexes **2**(Mo, W) Cr in solution spontaneously convert to **3**(Mo, W) Cr upon standing at ambient light and temperature, but those



complexes with $M' = \text{Mo}, \text{W}$ (**2**(Mo, W) M') need either stronger UV irradiation or warming for the analogous transformations to **3**(Mo, W) M' . All monobridged complexes **2** are light reddish-brown solids, and the dibridged compounds **3** are the orange solids, which are air-stable for several days but they decompose rapidly in solution exposed to the air.

Spectroscopy. ^1H and ^{31}P NMR and IR data for new complexes **2** and **3** together with those for metallophosphines **1**(Mo, W) are given in Table 3. ^1H resonances show a systematic deshielding of cyclopentadienyl protons on going from the terminal phosphido complexes **1**, through the monobridged bimetallics **2**, to the dibridged ones **3**. As expected the resonances of bridging hydride ligands in dibridged complexes **3** are recorded at higher fields than those observed for terminal hydrides in monobridged derivatives **2**.

Three principal trends in the ^{31}P chemical shifts are apparent from Table 3: (i) lower fields are observed for all molybdenocene complexes (**1–3**) Mo than for those of tungstenocene (**1–3**) W ; (ii) the shifts depend on the metal M' , and move downfield in the order $\text{W} > \text{Mo} > \text{Cr}$ in complexes **2** and **3**; and (iii) with the same metals M and M' , the resonances for dibridged complexes **3** are shifted by some 100 ppm to lower fields with respect to the monobridged complexes **2**.

IR spectra in carbonyl stretching region, $\nu(\text{CO})$, exhibit the patterns typical of $M'(\text{CO})_5$ (complexes **2**) and $M'(\text{CO})_4$ (complexes **3**) fragments. Their most important feature consists of the rather low energies compared to other known $M(\text{CO})_n$ systems.

X-ray Structure. The crystal structure of **3WW** is built of discrete dinuclear organometallic molecules without unusual intermolecular contacts. The metallic atoms are bridged by one PPh_2 ligand and one not located hydride ligand (Figure 1). The presence of this hydride bridge is however easily found out from the overall geometry of the molecule. One tungsten center (W^{IV}) shows the usual distorted tetrahedral geometry typical of bent metallocenes whereas the coordination geometry about the second tungsten center (W^{O}) is octahedral. A direct metal–metal interaction is suggested from the observed W–W distance of $3.271(1) \text{ \AA}$ and the EHMO calculations.

Table 3. NMR (^1H and ^{31}P)^a and IR^b Spectroscopic Data

		^1H (Cp)	J_{PH}	^1H (H^-)	J_{PH}	J_{WH}	^1H (Ph)	^{31}P	J_{PW}	ν_{CO}
Metallophosphines										
$\text{Cp}_2\text{Mo}(\text{PPh}_2)(\text{H})$	1a	4.69 (d)	1.5	−7.65 (d)	31.5		7.53–6.83 (m)	−10.3 (s)		
$\text{Cp}_2\text{W}(\text{PPh}_2)(\text{H})$	1b	4.65 (d)	1.5	−11.26 (d)	24.0	79	7.57–6.81 (m)	−46.3 (s)		
Monobridged Complexes										
$\text{Cp}_2\text{Mo}(\text{H})(\mu\text{-PPh}_2)\text{Cr}(\text{CO})_5$	2aCr	4.87 (d)	1.9	−7.78 (d)	37.5		7.02–7.85 (m)	32.5 (s)	2046 (m), 1928 (s), 1896 (s)	
$\text{Cp}_2\text{Mo}(\text{H})(\mu\text{-PPh}_2)\text{Mo}(\text{CO})_5$	2aMo	4.85 (d)	1.8	−7.83 (d)	37		7.09–8.20 (m)	16.0 (s) ^c	2060 (m), 1931 (s), 1897 (s)	
$\text{Cp}_2\text{Mo}(\text{H})(\mu\text{-PPh}_2)\text{W}(\text{CO})_5$	2aW	4.88 (d)	1.8	−7.75 (d)	38		7.04–7.86 (m)	−10.3 (s)	183 2058 (m), 1924 (s), 1897 (s)	
$\text{Cp}_2\text{W}(\text{H})(\mu\text{-PPh}_2)\text{Cr}(\text{CO})_5$	2bCr	4.85 (d)	1.8	−11.24 (d)	31	83	6.99–7.91 (m)	−29.5 (s)	176 2046 (m), 1927 (s), 1897 (s)	
$\text{Cp}_2\text{W}(\text{H})(\mu\text{-PPh}_2)\text{Mo}(\text{CO})_5$	2bMo	4.82 (d)	1.8	−11.32 (d)	31	86	6.99–8.26 (m)	−36.0 (s)	172 2060 (m), 1933 (s), 1898 (s)	
$\text{Cp}_2\text{W}(\text{H})(\mu\text{-PPh}_2)\text{W}(\text{CO})_5$	2bW	4.85 (d)	1.8	−11.23 (d)	32	85	7.01–7.88 (m)	−50.0 (s) ^c	191 ^c 2058 (m), 1921 (s), 1895 (s)	
Dibridged Complexes										
$\text{Cp}_2\text{Mo}(\mu\text{-PPh}_2, \text{H})\text{Cr}(\text{CO})_4$	3aCr	4.93 (d)	1.9	−14.75 (d)	25		7.16–8.28 (m)	135.7 (s)	1987 (m), 1890 (s), 1868 (s), 1855 (s)	
$\text{Cp}_2\text{Mo}(\mu\text{-PPh}_2, \text{H})\text{Mo}(\text{CO})_4$	3aMo	4.97 (d)	2.4	−13.65 (d)	19.5		7.10–8.27 (m)	105.8 (s)	1999 (m), 1892 (s), 1880 (s), 1857 (s)	
$\text{Cp}_2\text{Mo}(\mu\text{-PPh}_2, \text{H})\text{W}(\text{CO})_4$	3aW	5.03 (d)	2.4	−13.16 (d)	16	<i>d</i>	7.22–8.20 (m)	97.0 (s)	255 1996 (m), 1887 (s), 1870 (s), 1852 (s)	
$\text{Cp}_2\text{W}(\mu\text{-PPh}_2, \text{H})\text{Cr}(\text{CO})_4$	3bCr	4.92 (d)	2.4	−17.52 (d)	17	57	7.11–8.30 (m)	92.6 (s)	208 1986 (m), 1888 (s), 1867 (s), 1852 (s)	
$\text{Cp}_2\text{W}(\mu\text{-PPh}_2, \text{H})\text{Mo}(\text{CO})_4$	3bMo	4.95 (d)	2.4	−16.67 (d)	12.2	<i>d</i>	6.97–8.29 (m)	63.1 (s)	194 1999 (m), 1892 (s), 1879 (s), 1854 (s)	
$\text{Cp}_2\text{W}(\mu\text{-PPh}_2, \text{H})\text{W}(\text{CO})_4$	3bW	5.01 (d)	1.8	−16.21 (d)	8	67, 33	7.17–8.23 (m)	50.3 (s) ^c	230 ^c 1995 (m), 1884 (s), 1868 (s), 1849 (s)	

^a In acetone-*d*₆, at ambient temperature, δ in ppm and J in Hz. ^b In THF, cm^{-1} . ^c Broad. ^d Not observed.

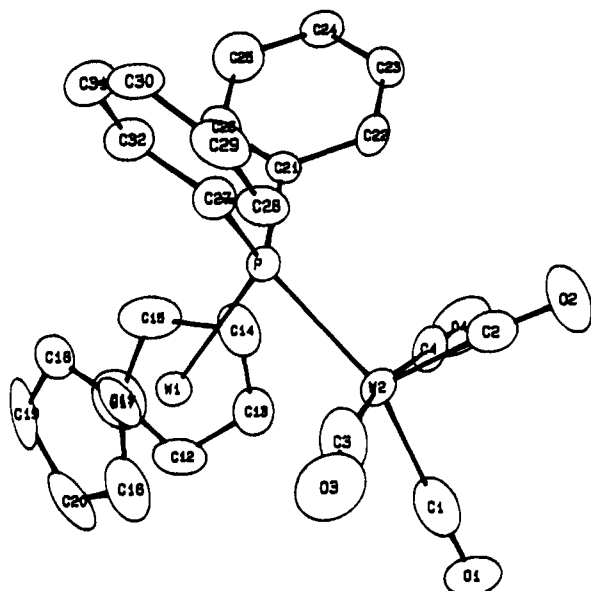


Figure 1. Molecular structure of for $\text{Cp}_2\text{W}(\mu\text{-PPH}_2,\text{H})\text{W}(\text{CO})_4$.

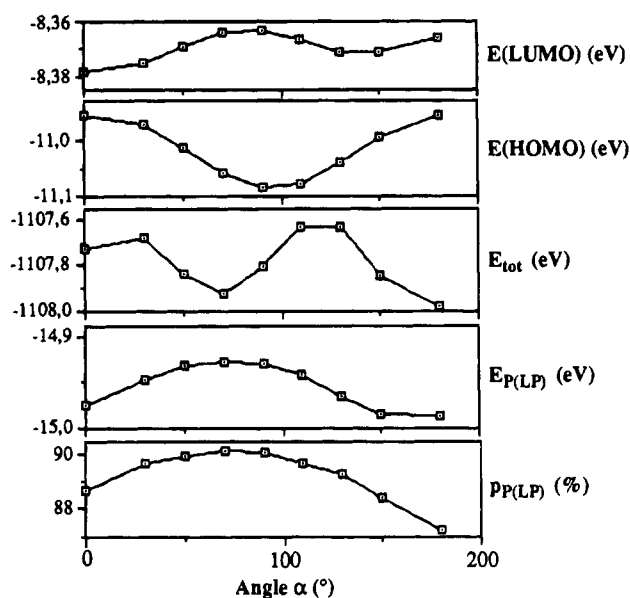


Figure 2. Behavior of the LUMO, HOMO, total energy, and phosphorus lone pair, as well as of the "p" character of this lone pair vs the dihedral angle α used for interpretation of the "transition metal gauche effect".

EHMO Calculations. The extended Hückel method was applied for two purposes: the understanding of electronic nature of the "transition metal gauche effect" and the estimation of electronic interactions between the molecular fragments in complexes 1, 2, and 3. The behavior of the most important parameters derived from this study, *i.e.* the energies of LUMO, HOMO, phosphorus atomic orbitals representing its lone pair, the *s/p* character of this lone pair and the total molecular energy as a function of the dihedral angle α , is presented in Figure 2. An analysis of this figure suggests that stable molecular

conformation and enhanced nucleophilicity of the phosphorus center correspond to a geometry for which the dihedral angle α is close to 75° . The results of fragment molecular orbital calculations concerning the electronic charges retained on $\text{Cp}_2\text{Mo}^{2+}$ fragment, and the energetics of its interaction with frontier molecular orbitals of $\text{H}(\text{PH}_2)\text{Mo}(\text{CO})_n$ ($n = 4$ and 5) fragments in complexes 1, 2, and 3, agree well with spectroscopic measurements. Relevant results of this study will be discussed at appropriate parts of the next section.

Discussion

Gauche Effect. The extremely easy reactions of metallo-phosphines 1 with metal carbonyl fragments focussed our attention on the electronic structures of complexes 1 and in particular on a quantitative approach to the nature of the "transition metal gauche effect". This effect in organometallic chemistry consists of an adoption of a molecular geometry in which the total energy and the repulsions between lone electronic pairs are minimized.

In the particular case of metallocenes with structures like 1 ($\text{M}^{\text{IV}}, d^2$),²⁹ several factors should be taken into account for understanding this effect. What happens when different conformations between the Cp_2M and PR_2 fragments are considered? How does the energy of the phosphorus lone pair, that of the metal (it is always the HOMO in the d^2 bent metallocenes known), and that of the LUMO (having the large contribution of metal atomic orbitals) vary with these conformations?

An inspection of Figure 2 shows that the energies of the LUMO and HOMO exhibit a maximum and a minimum near $\alpha = 90^\circ$, respectively. Even if the variation of energy of the LUMO is rather flat, the HOMO–LUMO energy gap indicates a preferential, mutually perpendicular orientation of the electronic lone pairs in complexes 1. Such a value of 90° seems to correspond to a pure gauche effect not affected by steric constraints.

The total energy curve shows two minima near 70° and 180° . The conformation corresponding to $\alpha = 180^\circ$ has never been observed in *diphenylphosphido* complexes. This minimum is certainly due to a disappearance of steric constraints upon substitution of small H atoms for bulkier phenyl groups in our model complex. However, such a conformation ($\alpha = 180^\circ$) may be expected for complexes with smaller *dimethylphosphido* ligands, and has been effectively observed in the structure of $\text{Cp}_2\text{Nb}(\text{CO})(\mu\text{-PMe}_2)\text{W}(\text{CO})_4(\text{PMe}_2\text{Ph})$.³⁰ Therefore, a conformation with α close to 70° should be the most stable one for metallocene–*diphenylphosphines*. It is worth to note, that it corresponds to the geometry we found in the niobiophosphine $\text{Cp}_2\text{Nb}(\text{CO})\text{P}^i\text{PrPh}$, where the LP(phosphorus)/LP(metal) dihedral angle (α) is equal to 74° .⁷ If we now look at the energies of the molecular orbitals representing the phosphorus LP,²⁷ we see that a maximum is observed for α angle close to $70\text{--}75^\circ$. The "p" character of this LP has a maximum in the same range. Thus, the enhanced nucleophilicity and reactivity of the phosphorus LP are due to an increase of energy of this lone pair as well as of its higher "p" character on going from the conformation with $\alpha = 0^\circ$ to the stable one with α close to

(24) Werner H.; Leonhard K.; Burschka Ch. *J. Organomet. Chem.* **1978**, *160*, 291.

(25) (a) Hoffmann, R. J. *J. Chem. Phys.* **1963**, *39*, 1397. (b) Hoffmann, R. J.; Lipscomb, W. N. *J. Chem. Phys.* **1962**, *36*, 2179. (c) Ammeter, J. H.; Burgi, H. B.; Thibeault, J. C.; Hoffmann, R. J. *J. Am. Chem. Soc.* **1978**, *100*, 3686. (d) FORTICON8, QCPE, PC version QCMP011.

(26) Standard H_{ii} values were used for C and H. P: $3s$ (-18.60), $\zeta_1 = 1.60$, $3p$ (-14.00), $\zeta_1 = 1.60$; Mo: $5s$ (-8.77), $\zeta_1 = 1.96$, $5p$ (-5.60), $\zeta_1 = 1.90$, $4d$ (-11.06), $\zeta_1 = 4.54$, $\zeta_2 = 1.90$, $C_1 = C_2 = 0.5899$.

(27) These are the orbitals No. 44, 51 and 52 with energies (eV) equal to -14.046 , -14.817 , and -15.975 , respectively, for $\alpha = 0$. The average values of $E_{P(LP)}$ used for plotting the corresponding curve in Figure 2 were calculated by weighting each individual value of energy with the coefficient of reduced charge matrix for phosphorus. The *s/p* character $pp_{(LP)}$ of phosphorus LP was calculated by using the squares of coefficients affecting the *s* and *p* atomic orbitals of phosphorus in molecular orbitals 44, 51, and 52.

(28) Mealli, C.; Proserpio, D. M. *J. Chem. Educ.* **1990**, *67*, 399.

(29) Lauher, J. W.; Hoffmann, R. J. *Am. Chem. Soc.* **1976**, *98*, 1729.

(30) Oudet P.; Kubicki M. M.; Moïse C. *Acta Crystallogr. Sect. C*, in press.

70–75°. The higher “p” character of phosphorus LP accounts for low energy of inversion barrier at phosphorus observed in terminal pyramidal phosphido complexes.^{5,7,31}

Spectroscopy. ¹H NMR. ¹H chemical shift values of cyclopentadienyl protons may provide useful probe for checking the electron density retained on bent Cp₂M (M = Mo, W, d²) fragment.³² The corresponding values are observed in the range of 4.88 to 4.82 ppm (in acetone d₆) for monobridged complexes **2** and are shifted downfield (5.03 to 4.92 ppm) for dibridged complexes **3**. These resonances are slightly affected by changing the M and M' metals. This suggests that the electron densities on Cp₂M fragments should be similar in all complexes **2** as well as in all complexes **3**. A comparison of ¹H (Cp) chemical shift values for **2** and **3** with those reported earlier for parent terminal phosphido complexes **1** (**1Mo** 4.69, **1W** 4.65 ppm)¹² indicates the following order of decreasing electron density retained on Cp₂M unit: **1** > **2** > **3**. The results of EHMO calculations carried out on the models of complexes **1**, **2**, and **3** agree with this order, because the calculated charges retained on Cp₂Mo fragment are equal to +0.921, +0.950 and +1.231, respectively.

The ¹H resonances of terminal hydride protons in monobridged complexes **2** are close to those observed in the parent metallophosphine **1** (Table 3). These resonances, as well as the ²J(PH) and ¹J(WH) (in tungstenocene series **2W**) coupling constants are essentially independent of the metal M' bound to phosphorus. The ²J(PH) couplings in **2MoM'** and **2WM'** are very close to those recorded for [Cp₂M(H)(PPh₂H)]⁺ parent complexes (35.0 and 26.4 Hz for Mo and W derivatives, respectively)¹¹ and the values of ¹J(WH) in **2WM'** (83–86 Hz) correspond very well to the couplings reported for terminal hydrides in other complexes derived from tungstenocene.³³ The ¹H hydride resonances in dibridged complexes **3** are observed at higher fields, as it is generally reported for protons in three-center M–H–M bonds, and show small but regular deshielding on going from M' = Cr to W. A similar deshielding has been already observed in monohydrido-bridged complexes Cp₂Ta(CO)(μ-H)M'(CO)₅ (M' = Cr, Mo, W).³⁴ The ²J(PH) couplings in complexes **3** are smaller than in **2** and decrease in the order of metals M', Cr > Mo > W. Likewise, the ²J(PH) and the ¹J(WH) couplings in tungstenocene complexes **3W** are smaller than in **2W** which may be attributed to an elongation of the Cp₂W–H distance when the hydride ligand forms a second bridge.

³¹P NMR. While the interpretation of ¹H chemical shifts may be roughly based on inductive effects and so correlated with the electron densities retained on the hydrogen atoms, it is well known that such an approach no longer holds for interpretation of ³¹P NMR resonances. The shielding depends mainly on the paramagnetic (σ_p) contribution to the overall screening, expressed by eq 3. The diamagnetic (inductive)

$$\sigma_p \approx -(\Delta E)^{-1} \langle r^{-3} \rangle (\sum Q) \quad (3)$$

contributions are considered to be roughly constant. ΔE is the mean energy of electronic excitation from the ground state to

the excited states, ⟨r⁻³⟩ are the radial expansions of non-s-orbitals, and ΣQ relates to the charge density/bond orders matrix (polarization term).

We have already mentioned that three principal trends of δ(³¹P) variations appear from data listed in Table 3: (i) lower fields are observed for all molybdenocene complexes (**1–3**)–Mo than for the tungstenocene ones (**1–3**)W; (ii) the shifts depend on the metal M', and move downfield in the order W > Mo > Cr in complexes **2** and **3**; and (iii) with the same metals M and M' the resonances for dibridged complexes **3** are shifted by some 100 ppm to lower fields with respect to the monobridged complexes **2**. Different metals have different shielding effects on the ³¹P nucleus, since at least two terms in eq 3 (ΔE and ⟨r⁻³⟩) are affected by a change of the metal. Thus, the consideration of these two contributions accounts exactly to the trends i and ii. The observed order agrees with the results obtained for M(CO)₅P and M(CO)₄P₂ phosphino complexes of Cr, Mo, and W,^{36,37} as well as for a number of diphenylphosphido-bridged compounds of the iron triad.^{1a} The occurrence of relativistic effects for heavier metals may explain the upfield shifts of the nuclei bound to them.³⁸ The ³¹P shift decreases (higher field) as the atomic number increases from top to bottom in a triad. The third trend may be understood on the basis of a simplified relation between the angular parameters at the phosphorus atom and the corresponding δ(³¹P): an angular constrain (closing of the M–P–M' angle) means a deshielding (decrease of ΔE, high negative value of σ_p, eq 3). The M–P–M' angles are close to 125° in diphenylphosphido-monobridged complexes Cp₂Mo(H)(μ-PPh₂)Mn(CO)₂Cp,¹² Cp₂Nb(CO)(μ-PMe₂)W(CO)₄(PMe₂Ph),³⁰ and Cp*₂Ta(CO)((μ-PPh₂)–Mn(CO)₂Cp,³⁹ but this angle is 81.6° in the dibridged structure of **3WW** discussed below.

Some information concerning the strengths of metal–phosphide (M'–P) bonds may be drawn from the values of coordination chemical shifts (Δ_c) defined as Δ_c = δ(³¹P)_{complex} – δ(³¹P)_{free ligand}.⁴⁰ If the metallophosphines **1** are considered as “free ligands”, their complexation on M'(CO)₅ fragment should modify a shielding of the ³¹P nuclei. The values of Δ_c extracted from Table 3 for monobridged complexes **2MoM'** are 42.8, 26.3, and 0.0 ppm for M' = Cr, Mo, and W, respectively. These Δ_c values are roughly 20 ppm smaller than those found for M'(CO)₅(PPh₃) complexes.^{37a} Thus, the M'–P bonds in Cp₂–Mo(H)(μ-PPh₂)M'(CO)₅ systems are weaker than the M'–P bonds in mononuclear complexes M'(CO)₅(PPh₃).

The ¹J_{PW} coupling constants in **2** and **3** fall well in the region of normal values observed for tungsten–phosphorus-bonded complexes (112–256 Hz).^{1c} These couplings are higher in dibridged complexes **3** than in monobridged **2** which may be explained by different strength of the M'(W)–P bonds. They should be longer and weaker in complexes **2W** (like in **2MoMn**) than in **3W** (see the discussion of the structure of **3WW** below).

It is well documented, that a deshielding of ³¹P resonances in phosphido bridged complexes may indicate a presence of a metal–metal bond. Thus, we would like at first to compare

- (31) (a) Buhro, W. E.; Gladysz, J. A. *Inorg. Chem.* **1985**, *24*, 3505. (b) Crisp, G. T.; Salem, G.; Wild, S. B.; Stephens, F. S. *Organometallics*, **1989**, *8*, 2360. (c) Malish, W.; Maish, R.; Meyer, A.; Greissinger, D.; Gross, E.; Colquhoun, I. J.; McFarlane, W. *Phosphorus Sulfur* **1983**, *18*, 299.
- (32) Kubicki, M. M.; Kergoat, R.; Guerchais, J. E.; Bkouche-Waksman, I.; Bois, C.; L'Haridon, P. *J. Organomet. Chem.* **1981**, *219*, 329.
- (33) Legzdins, P.; Martin, J. T.; Einstein, F. W. B.; Willis, A. C. *J. Am. Chem. Soc.* **1986**, *108*, 7971.
- (34) Reynoud, J.-F.; Leblanc, J.-C.; Moïse, C. *J. Organomet. Chem.* **1985**, *296*, 377.

- (35) Letcher, J. H.; Van Wazer, J. R. *J. Chem. Phys.* **1966**, *44*, 815.
- (36) Nixon, J. F.; Pidcock, A. In *Annual Review of NMR Spectroscopy*; Mooney, E., Ed.; Academic Press: London, 1969; Vol. 2, p 346.
- (37) (a) Grim, S. O.; Wheatland, D. A.; McFarlane, W. *J. Am. Chem. Soc.* **1967**, *89*, 5573. (b) Grim, S. O.; Del Gaudio, J.; Molenda, R. P.; Tolman, C. A.; Jesson, J. P. *J. Am. Chem. Soc.* **1974**, *96*, 3416. (c) Grim, S. O.; Briggs, W. L.; Barth, R. C.; Tolman, C. A.; Jesson, J. P. *Inorg. Chem.* **1974**, *13*, 1095.
- (38) Pyykkö, P.; Görling, A.; Rösch, N. *Mol. Phys.* **1987**, *61*, 195.
- (39) Bonnet, G.; Lavastre, O.; Kubicki, M. M.; Moïse, C. *Acta Crystallogr., Sect. A*, **1990**, *A46 Suppl.*, C227.
- (40) Mann, B. E.; Masters, C.; Shaw, B. L.; Stainbank, R. E. *Inorg. Nucl. Chem. Lett.* **1971**, *7*, 881.

our ^{31}P data with those reported for the closely related structures of Pt/Ru^{14} and Mo/Mo and W/W^{15} bimetallics.

The diphenylphosphido bridged Pt–Ru heterobimetallic system: **2PtRu** ($[\text{Cp}(\text{CO})_2\text{Ru}(\mu\text{-PPh}_2)\text{PtH}(\text{PPh}_3)_2]^+$), **3PtRu** ($[\text{Cp}(\text{CO})\text{Ru}(\mu\text{-PPh}_2,\text{H})\text{Pt}(\text{PPh}_3)_2]^+$), and metal–metal bonded complex **Pt–Ru** ($[\text{Cp}(\text{CO})\text{Ru}(\mu\text{-PPh}_2)\text{Pt}(\text{PPh}_3)_2]$) have been studied by Powell.¹⁴ The ^{31}P resonances are reported at -11 , $+167$, and $+160$ ppm for **2PtRu**, **3PtRu**, and **Pt–Ru**, respectively. That, observed for **2PtRu** is the same as our value for **2MoW** (Table 3). However, a deshielding upon the formation of hydride bridge is of ~ 170 ppm in **3PtRu** and only of 107 ppm for **3MoW**. It is interesting to note that the ^{31}P resonances in Powell's complexes **3PtRu** and **Pt–Ru** are quite similar, the higher field even being observed for metal–metal bonded complex **Pt–Ru**. This may be interpreted as resulting from similar angular parameters on the phosphorus atom in **3PtRu** and **Pt–Ru**, or as indicative of Pt–Ru direct interactions in hydrido-bridged **3PtRu**. Higher deshielding of ^{31}P nuclei in dibridged complex **3PtRu** than in **3MoW** may result from the differences of coordination numbers of Pt, equal to four in **3PtRu**, but formally equal to eight for M in $\text{Cp}_2\text{M}(\text{H})(\text{PPh}_2)$ fragment of our complexes **2** and **3**, and from the difference of covalent radii of Pt(II) and M(IV) ($\text{M} = \text{Mo}, \text{W}$). Thus, even if the overall type of electronic interactions in the $\text{M}(\mu\text{-H},\text{PPh}_2)\text{-M}'$ core of molecules **3** may be similar in our complexes and in those of Powell, the ^{31}P nuclei may be more sensitive to the structural changes in the Pt–Ru series because of the shorter Pt–P bond.

Another interesting comparison of ^{31}P data for our complexes **2** and **3** can be made with those studied by Calligaris and Wojcicki¹⁵ in reduction chemistry of $\text{M}_2(\text{CO})_8(\mu\text{-PPh}_2)_2$ ($\text{M} = \text{Mo}, \text{W}$), namely the monobridged complexes *with* $[(\text{CO})_4\text{M}(\mu\text{-PPh}_2)\text{M}(\text{CO})_4(\text{PPh}_2\text{H})]^-$ and *without* a metal–metal bond $[(\text{CO})_5\text{M}(\mu\text{-PPh}_2)\text{M}(\text{CO})_4(\text{PPh}_2\text{H})]^-$. In the complexes without an M–M bond the ^{31}P chemical shifts of bridging phosphorus atoms are -22.1 ppm ($\text{M} = \text{Mo}$) and -61.1 ppm ($\text{M} = \text{W}$) and are shifted downfield in those with M–M bond viz $+106$ ppm ($\text{M} = \text{Mo}$) and $+85$ ppm ($\text{M} = \text{W}$). Thus, the formation of the metal–metal bond is accompanied here by a deshielding of $128\text{--}146$ ppm. A comparison of deshieldings of ^{31}P nuclei in the complexes of Powell and of Calligaris and Wojcicki with the values observed in our complexes **3** ($90\text{--}122$ ppm with respect to compounds **2**) may indicate the presence of metal–metal interactions in the series of complexes **3**.

IR. Higher frequencies of $\nu(\text{CO})$ stretching vibrations are observed in **2** than in **3** (Table 3) indicating higher electron density on carbonyl groups in the later compounds. There is a highly pronounced red shift of these frequencies in $\text{W}(\text{CO})_4$ units of **3(Mo,W)W** with respect to the values observed for *cis*- $\text{W}(\text{CO})_4(\text{PPh}_2\text{H})_2$ ⁴¹ -2022 , 1928 , 1905 and 1890 cm^{-1} . On the other hand the blue shifts ($20\text{--}40$ cm^{-1} vs *cis*- $\text{W}(\text{CO})_4(\text{PPh}_2\text{H})_2$) were observed in the complexes with two bridging phosphido ligands in group 4–group 6 bimetallics⁴¹ and in the compounds with tungsten to late transition metal bond $(\text{CO})_4\text{W}(\mu\text{-PPh}_2)_2\text{Pt}(\text{PPh}_3)$ ⁴² and $(\text{CO})_4\text{W}(\mu\text{-PPh}_2)_2\text{Ir}(\text{H})(\text{CO})(\text{PPh}_3)$ ⁴³. The red shift observed in complexes **3(Mo,W)W** indicates that a significant electron density is transferred from the Cp_2M fragment to the $\text{W}(\text{CO})_4$ fragment either simply through the bridging ligands or with the assistance of a metal–metal interaction. The EHMO calculations, carried out on the models

Table 4. Selected Interatomic Distances (Å) and Angles (deg) for $\text{Cp}_2\text{W}(\mu\text{-PPh}_2,\text{H})\text{W}(\text{CO})_4$ ^a

W1···W2	3.2708(8)
W1–CP1	1.97
W1–CP2	1.97
W1–P	2.540(5)
W2–P	2.464(3)
W2–C1	1.94(2)
W2–C2	1.94(2)
W2–C3	2.00(2)
W2–C4	1.98(2)
W1–P–W2	81.6(1)
CP1–W1–CP2	137.1
P–W1–CP1	110.8
P–W1–CP2	107.7
P–W2–C1	161.4(6)
P–W2–C2	105.2(5)
P–W2–C3	97.4(5)
P–W2–C4	91.8(4)
C1–W2–C2	93.5(7)
C3–W2–C4	169.9(6)

^a CP1 and CP2 are the gravity centers of C11–C15 and C16–C20 rings, respectively.

of **2MoMo** and **3MoMo** with $\text{Cp}_2\text{Mo}(\text{H})(\text{PH}_2)$ fragment and $\text{Mo}(\text{CO})_5$ and $\text{Mo}(\text{CO})_4$ ones, gave the net charges retained on penta- and tetracarbonyl molybdenum moieties equal to -0.505 and -1.080 , respectively. Thus, it may be assumed that the $\text{Mo}(\text{CO})_4$ unit accepts more electron density than does $\text{Mo}(\text{CO})_5$ entity. The $\nu(\text{CO})$ frequencies in **3(Mo,W)Mo** complexes are only slightly higher than in the mononuclear compounds $(\text{CO})_4\text{Mo}(\text{N–N})$ with strong donor saturated chelates.⁴⁴

Molecular Structure of $\text{Cp}_2\text{W}(\mu\text{-PPh}_2,\text{H})\text{W}(\text{CO})_4$ (3WW**).** An ORTEP drawing of **3WW** giving the atom labeling scheme is shown in Figure 1. Relevant bond distances and angles are set out in Table 4. Two geometric parameters dramatically change when one compares the structure of **3WW** with that of monobridged complex $\text{Cp}_2\text{Mo}(\text{H})(\mu\text{-PPh}_2)\text{Mn}(\text{CO})_2\text{Cp}$,¹² **2Mo–Mn**: the $\text{M}'\text{–M}$ separation and $\text{M–P–M}'$ angle decrease from $4.391(1)$ to $3.271(1)$ Å and from $124.5(1)$ to $81.6(1)^\circ$, respectively.

The W–W distance of $3.271(1)$ Å in the structure of **3WW** is slightly longer than the values of metal–metal bond lengths observed in the dimers of formula $[(\text{C}_5\text{H}_5)(\text{CO})_3\text{W}]_2$ ($3.222(1)$ Å),⁴⁵ phosphinidene bridged $(\mu\text{-PR})[\text{Cp}(\text{CO})_2\text{W}]_2$ ($3.251(1)$ Å),⁴⁶ and $[\text{W}(\text{CO})_4(\mu\text{-PPh}_2)]_2$ ($3.0256(4)$ Å).¹⁵ It is however shorter than the values of ca. $3.3\text{--}3.4$ Å observed in hydrido bridged W–W carbonyl-nitrosyl complexes, where metal–metal interactions are not excluded.⁴⁷ Is this distance really suggesting of a W–W bond? The question of direct metal–metal bonding in doubly bridged compounds is still controversial since the bonding interactions between the metals may take place through orbitals involving the bridging atoms.^{42,48} The nature of direct bonding is a formal concept adjusted in order to comply with the 18 electron rule, spin state, and metal–metal distance.⁴⁹ This question has been often invoked in phosphido bridged compounds of the type $\text{Cp}_2\text{M}(\mu\text{-PR})_2\text{M}'(\text{CO})_4$ ($\text{M}' = \text{Cr}, \text{Mo}, \text{W}$)

(44) Shiu, K. B.; Wang, S. L.; Liao, F. L. *J. Organomet. Chem.* **1991**, *420*, 207.

(45) Adams, R. D.; Collins, D. M.; Cotton, F. A. *Inorg. Chem.* **1974**, *13*, 1086.

(46) Arif, A. M.; Cowley, A. H.; Norman, N. C.; Orpen, A. G.; Pakulski, M. *Organometallics* **1988**, *7*, 309.

(47) (a) Lin, J. T.; Chang, K.-Y.; Wang, S. Y.; Wen, Y. S.; Tseng, L.-H.; Chang, C.-C.; Peng, S.-M.; Weng, Y.; Lee, G. H. *Organometallics* **1991**, *10*, 2377. (b) Lin, J. T.; Huang, P. S.; Tsai, T. Y. R.; Liao, C.-Y.; Tseng, L.-H.; Wen, Y. S.; Shi, F. K. *Inorg. Chem.* **1992**, *31*, 4444.

(48) (a) Bénard, M.; Dedieu, A.; Nakamura, S. *Nouv. J. Chim.* **1884**, *8*, 149. (b) Bénard, M. *Inorg. Chem.* **1979**, *18*, 2782.

(41) Targos, T. S.; Rosen, R. P.; Whittle, R. R.; Geoffroy, G. L. *Inorg. Chem.* **1985**, *24*, 1375.

(42) Morrison, E. D.; Harley, A. D.; Marcelli, M. A.; Geoffroy, G. L.; Rheingold, A. L.; Fultz, W. C. *Organometallics* **1984**, *3*, 1407.

(43) Breen, M. J.; Shulman, P. M.; Geoffroy, G. L.; Rheingold, A. L.; Fultz, W. C. *Organometallics* **1984**, *3*, 782.

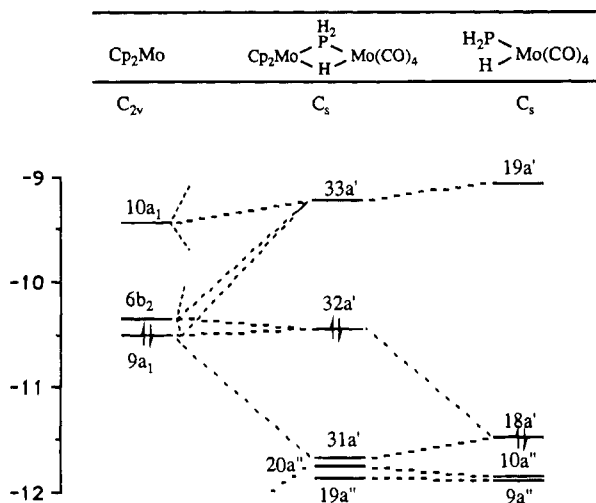


Figure 3. Correlation diagram for dibridged complexes (3) showing a metal-metal interaction.

derived from group 4 metallocenes where the formal electron count gives $16e^-$ for M and $18e^-$ for M'. In **3WW** both tungsten atoms ($18e^-$) bear formally the lone electron pairs in nonbonding molecular orbitals rendering metal-metal interactions somewhat doubtful. However, the observed M-M' separation is compatible with the corresponding distances (3.289(1)–3.400(1) Å) found in diphosphido-bridged complexes of group 4 metallocenes (Cp_2M , M = Zr, Hf) with group 6 metal carbonyls ($M'(CO)_4$, M = Mo, W).^{13,41,50} The weak metal-metal dative bonding from $M'(CO)_4$ ($18e^-$, d^0) to Cp_2M ($16e^-$, d^0) has been suggested for these compounds. Another example of dative metal to metal bond is found in the structure of $Cp(CO)_2W(\mu-PPh_2)Cr(CO)_5$ ¹⁹, in which the $Cr^0(18e^-)-W^{II}(16e^-)$ distance is equal to 3.089(1) Å. Taking into account a difference of covalent radii (W^0 vs. $Cr^0 = 0.14 \text{ Å}^{51}$), our W-W distance is only 0.04 Å longer. Analogous dative bonds from $W^0(18e^-)$ to Re^I (3.111(1) Å)⁵² and Re^{III} (3.105(1) Å)⁵³ ($16e^-$) have been reported. Thus, although our W-W separation of 3.271(1) Å after correction for differences of covalent radii of group 4, 6, and 7 metals, may appear slightly longer than the values cited above, the presence of direct interactions between the filled orbitals of both W atoms should not be ruled out. The interaction diagram of frontier orbitals in a model complex of **3**, and the shapes of resulting molecular orbitals (HOMO and SOMO) are shown in Figures 3 and 4. The HOMO, which has a major contribution from molybdenum atom of Cp_2Mo fragment (80% Mo1, 10% Cp, 5% Mo2, 5% CO) and an antibonding metal-metal character, is slightly destabilized ($\approx 0.08 \text{ eV}$) with respect to the energy of the HOMO in Cp_2Mo fragment. However, the SOMO, which is mainly built of $Mo(CO)_2$ (CO's trans to P and H) orbitals (50% Mo2, $\approx 20\%$ of each CO, 10% of Mo1) is metal-metal bonding and is stabilized by $\approx 0.24 \text{ eV}$ with respect to its energy in $Mo(CO)_4$ fragment. The net overlap population of Mo1-Mo2 atoms is positive (0.039). Note, that even the negative values of direct metal-metal overlap have been considered as representing a metal-

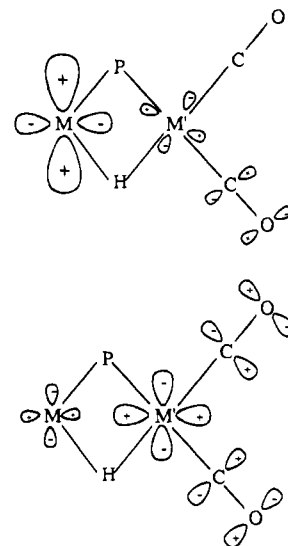


Figure 4. Shapes of the HOMO (top) and SOMO (bottom) molecular orbitals in dibridged complexes (3).

metal interaction in $Cp_2Th(\mu-PH_2)_2Ni(CO)_2$,⁵⁴ and that the presence of $Zr^{III}-Zr^{III}$ bonding interaction in $[Cp_2Zr(\mu-X)]_2$ (X = PMe_2 , I) dimers has been confirmed by theoretical studies⁵⁵ for very long Zr-Zr distance of 3.653 Å.⁵⁶

The W-P-M angle of $81.6(1)^\circ$ falls in the range of $79-83^\circ$ observed for Zr(Hf)-W(Mo) heterobimetallics, but is clearly smaller than in $[W_2(CO)_8(\mu-PPh_2)_2]^{2-}$ (104.2°)¹⁵ and $[Fe_2(CO)_6(\mu-PPh_2)_2]^{2-}$ (105.5°)⁵⁷ anions without metal-metal interactions. The steric repulsions observed between Cp_2MoH and $Mn(CO)_2Cp$ fragments in **2MoMn** complex are weaker or no longer exist in **3WW**, as indicated by the shorter W1-P of 2.540(5) Å (2.602(2) Å in **2MoMn**) and W2-P of 2.464(3) Å distances than those observed in **2MoMn**. The Mn-P bond length in **2MoMn** is equal to 2.359(2) Å but taking into account the difference of covalent radii of W^0 and Mn^I equal to 0.23 Å,⁵¹ the W2-P bond in **3WW** must be considered as a stronger one. This W2-P bond is also shorter than the W-P distances observed in a number of diphosphido bridged complexes $(CO)_4W(\mu-PR_2)M'Ln$ with or without metal-metal bond (2.474–2.536 Å) and in *cis*-(CO)₄M(PR_3)₂ mononuclear ones (2.522–2.577 Å).⁵⁸ The bridging PPh_2 and H ligands seem to exert a similar trans-influence on the carbonyl ligands. The W2-C1 (*trans* to P) and W2-C2 (*trans* to H) bond lengths are equal to 1.94(2) Å and are shorter than the *cis* W2-C distances (mean value 1.99(2) Å). Both the *cis* and the *trans* W-C bonds in the structure of **3WW** are shorter than those found in some typical mononuclear *cis*- $L_2M(CO)_4$ (M = Mo, W) tetracarbonyls: *ca.* 1.97–1.98 and 2.02–2.03 Å, respectively.^{58,59} This structural observation indicates a high electron density retained on $W(CO)_4$ fragment in the complexes **3(Mo,W)M'** and confirms the low frequencies of $\nu(CO)$ vibrations observed on IR spectra.

(49) (a) Cotton, F. A.; Jamerson, J. D. *J. Am. Chem. Soc.* **1976**, *98*, 5396. (b) Jemmis, E. D.; Pinhas, A. R.; Hoffmann, R. *J. Am. Chem. Soc.* **1980**, *102*, 2576.
 (50) (a) Gelmini, L.; Matassa, L. C.; Stephan, D. W. *Inorg. Chem.* **1985**, *24*, 2585. (b) Zheng, P. Y.; Nadashi, T.; Stephan, D. W. *Organometallics* **1989**, *8*, 1393.
 (51) Churchill, M. R. *Perspect. Struct. Chem.* **1971**, *3*, 91.
 (52) Mercer, W. C.; Whittle, R. R.; Burkhardt, E. W.; Geoffroy, G. L. *Organometallics* **1985**, *4*, 68.
 (53) Mercer, W. C.; Geoffroy, G. L.; Rheingold, A. L. *Organometallics* **1985**, *4*, 1418.

(54) Ortiz, J. V. *J. Am. Chem. Soc.* **1986**, *108*, 550.
 (55) (a) Rohmer, M.-M.; Bénard, M. *Organometallics* **1991**, *10*, 157. (b) DeKock, R. L.; Peterson, M. A.; Reynolds, L. E. L.; Chen, L.-H.; Baerends, E. J.; Vermooijs, P. *Organometallics* **1993**, *12*, 2794.
 (56) Chiang, M. Y.; Gambarotta, S.; van Bolhuis, F. *Organometallics* **1988**, *7*, 1864.
 (57) Ginsburg, R. E.; Rothrock, R. K.; Finke, R. G.; Collman, J. P.; Dahl, L. F. *J. Am. Chem. Soc.* **1979**, *101*, 6550.
 (58) Powell, J.; Couture, C.; Gregg, M. R.; Sawyer, J. F. *Inorg. Chem.* **1989**, *28*, 3437 and references therein.
 (59) (a) Churchill, M. R.; Rheingold, A. L.; Keiter, R. L. *Inorg. Chem.* **1981**, *20*, 2730. (b) Cotton, A. F.; Daresbourg, D. J.; Klein, S.; Kolthammer, B. W. S. *Inorg. Chem.* **1982**, *21*, 1651. (c) Varshney, A.; Gray, G. M. *Inorg. Chem.* **1991**, *30*, 1748. (d) Ueng, C.-H.; Leu, L.-C. *Acta. Crystallogr. Sect. C* **1991**, *C47*, 725.

The CP1–W1–CP2 angle of 137.1° is smaller than the CP1–Mo–CP2 angle of 139.8° in **2MoMn** complex. This indicates a weaker repulsion between the rings and thus a lower electron density retained on the Cp₂M fragment in complexes **3** (e.g. **3WW**) than on the Cp₂M part of the monobridged complexes **2** (e.g. **2MoMn**) and agrees with ¹H NMR data and with EHMO calculations.

Conclusions

New series of dinuclear complexes with one phosphido bridge (**2**) and with phosphido and hydrido bridges (**3**) have been prepared from metallophosphines Cp₂M(H)(PPh₂) (M = Mo, W) (**1**) in which the phosphorus atom exhibits a high nucleophilicity. This last is enhanced by the repulsive interaction of the phosphorus lone pair with a well defined HOMO nonbond-

ing molecular orbital of metallocene fragment (transition metal gauche effect). Thus, the chemistry presented in this paper would *a priori* be expected. We focussed our attention on the electronic properties of complexes **1**, **2**, and **3**. A good and logical agreement of results obtained by different methods (¹H and ³¹P NMR, IR, EHMO and X-rays) is observed. An interesting conclusion concerns the electron density retained on M'(CO)_n fragments: it is higher in tetracarbonyl moieties (complexes **3**) than in pentacarbonyl ones (complexes **2**). The presence of direct metal–metal interaction in **3** can account for this fact.

Supplementary Material Available: Tables of elemental analytical data, anisotropic thermal parameters, hydrogen atom coordinates, complete bond distances and angles, and least-squares planes (7 pages). Ordering information is given on any current masthead page.